

## RAPID COMMUNICATION

## Volumetric Analysis of Medial Temporal Lobe Subregions in Developmental Amnesia using High-Resolution Magnetic Resonance Imaging

Rosanna K. Olsen,<sup>1\*</sup> Daniela J. Palombo,<sup>1,2</sup> Jennifer S. Rabin,<sup>3</sup> Brian Levine,<sup>1,2,4</sup>  
Jennifer D. Ryan,<sup>1,2,5</sup> and R. Shayna Rosenbaum<sup>1,3,6</sup>

**ABSTRACT:** There is great interest in the cognitive consequences of hippocampal volume loss in developmental amnesia (DA). In many DA cases, volume loss occurs before the hippocampus is fully developed, and yet little is known about the locus, extent, and distribution of damage in these cases. We used high-resolution MRI to manually segment the medial temporal lobe (MTL) subregions in H.C., an adult with DA, and a group of sex-, age- and education-matched control participants ( $n = 10$ ). The hippocampus was defined and divided into anterior (head) and posterior (body and tail) segments. Within the body of the hippocampus, the subregions (CA<sub>1</sub>, DG/CA<sub>2/3</sub>, and subiculum) were defined. Finally, the entorhinal (ERC), perirhinal (PRC), and parahippocampal (PHC) cortices were segmented. Anterior hippocampus was reduced bilaterally and posterior hippocampus was significantly reduced on the right. In the body of the hippocampus, all three subregions were reduced in the left hemisphere, whereas CA<sub>1</sub> and subiculum were reduced in the right hemisphere. No group differences were observed in the PRC and ERC, whereas left PHC volume was marginally increased in H.C. compared to controls. These results can be used to inform patterns of spared and impaired cognitive abilities in DA and perhaps in amnesia more generally. © 2013 The Authors. Hippocampus Published by Wiley Periodicals, Inc.

**KEY WORDS:** patient H.C.; CA<sub>1</sub>; dentate gyrus; CA<sub>3</sub>; subiculum

Our understanding of hippocampal function and dissociations in memory has been illuminated by studies of individuals with early-onset hippocampal volume loss, commonly due to anoxia, known as

having “developmental amnesia” (DA). Seminal research by Vargha-Khadem et al. (1997), including careful study of the single case Jon, provided important insights about the relative role of the hippocampus in episodic memory and related recollection of recognized items and events versus semantic memory and related familiarity-based recognition (Baddeley et al., 2001). Based on group analysis of whole-brain structural MRI using voxel-based morphometry (VBM), this pattern has been attributed to volume loss in the MTL—specifically to the hippocampus—although changes in the putamen, posterior thalamus, and retrosplenial cortex were also noted (Vargha-Khadem et al., 2003). Hippocampal tracings were consistent with the VBM results: hippocampal volumes were estimated to be 30–54% reduced from normal. Nonetheless, surprisingly little is known about whether this loss is concentrated within selective subregions and/or the extent to which damage is distributed along the anterior–posterior axis.

A critical next step in the study of DA is the elucidation of the particular hippocampal subregions that are affected *in vivo*. Post-mortem studies of individuals with amnesia due to late-life ischemia have indicated relatively selective cell loss in the CA<sub>1</sub> region (Zola-Morgan et al., 1986). Similarly, *in vitro* studies have documented differential effects of anoxia on hippocampal subregions CA<sub>1</sub> and CA<sub>3</sub>—that is, CA<sub>1</sub> cells appear to be more sensitive to hypoxia damage than CA<sub>3</sub> cells (Kawasaki et al., 1990). More recently, a qualitative analysis of high-resolution MRI images of the MTL in a case of amnesia of mixed etiology (adult-onset anoxia and adolescent-onset epilepsy) suggested selective reduction of CA<sub>1</sub> in the right hippocampus but more extensive damage to the left hippocampus that appears to have encompassed all subregions. Visual inspection of the images also suggested reduction of the anterior portion of the parahippocampal gyrus bilaterally as well as the left fimbria and left mammillary body (Warren et al., 2012). High-resolution structural imaging techniques, combined with quantitative volumetric comparisons

This is an open access article under the terms of the Creative Commons Attribution-NonCommercial-NoDerivs License, which permits use and distribution in any medium, provided the original work is properly cited, the use is non-commercial and no modifications or adaptations are made.

<sup>1</sup>Rotman Research Institute at Baycrest, Toronto, Ontario, Canada; <sup>2</sup>Department of Psychology, University of Toronto, Toronto, Ontario, Canada; <sup>3</sup>Department of Psychology, York University, Toronto, Ontario, Canada; <sup>4</sup>Department of Medicine (Neurology), University of Toronto, Toronto, Ontario, Canada; <sup>5</sup>Department of Psychiatry, University of Toronto, Toronto, Ontario, Canada; <sup>6</sup>Neuroscience Graduate Diploma Program, York University, Toronto, Ontario, Canada

Grant sponsor: Ontario Ministry of Economic Development and Innovation Early Researcher Award (to R.S.R.); Grant sponsor: Canadian Institutes of Health Research (CIHR) Operating grant (to R.S.R. and B.L.); Grant number: MOP-93535; Grant sponsor: CIHR Young Investigator Award (to R.S.R.), Canadian Research Chair Award (to J.D.R.); Grant sponsor: CIHR Operating grant (to B.L.); Grant number: OMP-62963.

\*Correspondence to: Rosanna K. Olsen, Rotman Research Institute, Baycrest 3560 Bathurst Street, Toronto, ON M6A 2E1, Canada. E-mail: rolsen@research.baycrest.org

Accepted for publication 24 May 2013.

DOI 10.1002/hipo.22153

Published online 5 July 2013 in Wiley Online Library (wileyonlinelibrary.com).

of amnesic individuals and matched controls, allow for differentiation among hippocampal subregions and could provide a richer understanding of how the behavioral profiles observed in individuals with hippocampal damage relate to their underlying brain pathology.

To this end, manual segmentation of the hippocampus and adjacent regions of MTL cortex was performed using high-resolution MRI of H.C., another well-documented case of DA. H.C. is a woman, aged 22 yrs at time of testing, whose memory impairment is likely a result of a perinatal brain injury. H.C. was born prematurely (gestational age = 32 weeks), and suffered hypoxia around the time of her birth. Like Jon, H.C. has impaired memory for personal life events, and this impairment extends to memory for public event details (Rosenbaum et al., 2011), but not to personal and general semantic memory. A parallel pattern of worse recollection than familiarity of recognized items was demonstrated on laboratory tests of episodic memory, though both processes appeared to have been affected in H.C., raising the possibility of additional volume loss in perirhinal cortex. Moreover, given previous reports of both episodic and spatial memory impairments in cases of DA, as well as impairments reflecting both “coarse” and “detailed” memories, volume reductions along the extent of the anterior–posterior axis of the hippocampus were expected in H.C. (Poppenk et al., 2013).

Despite H.C.’s lack of recollection for both personal and public events, she is an otherwise healthy individual who completed high school, 1 year of technical college, and 1 year of a post-secondary culinary program (years of education = 14; for full neuropsychological profile, see Hurley et al., 2011; Rosenbaum et al., 2011). Ten typically developing participants (all female; mean age = 19.40, SD = 1.51; mean years of education = 13.60, SD = 0.97) with no history of psychiatric or neurological illness served as controls. All participants provided informed consent. This study was approved by the Baycrest and York University Research Ethics Boards.

Structural MRI images were acquired using a 3T Siemens Trio scanner. A whole-brain T1-weighted MPRAGE sequence (TE/TR = 2.63 ms/2000 ms, 176 oblique axial slices,  $256 \times 192$  matrix, voxel size =  $1 \text{ mm}^3$ , FOV = 256 mm) was collected. This image was used to obtain a measure of total brain volume and for confirmation of anatomical boundaries best viewed in the sagittal and/or axial plane. For later segmentation, a second high-resolution T2-weighted structural image was acquired in an oblique coronal plane, perpendicular to the long axis of the hippocampus (TE/TR = 68 ms/3000, 22–28 slices,  $512 \times 512$  matrix, voxel size of  $0.43 \times 0.43 \times 3 \text{ mm}$ , no skip, FOV = 220 mm).

Regions-of-interest (ROI) were defined manually in native space using FSLview (v. 3.0.2) by the first author. Segmentation procedures were based on established procedures (Olsen et al., 2009) and published hippocampal atlases and protocols (Insausti et al., 1998; Pruessner et al., 2002; Duvernoy, 2005; Mueller et al., 2007; Yushkevich et al., 2009). In the body of the hippocampus, where the vestigial hippocampal sulcus appears as a dark band, the CA<sub>1</sub>, subiculum, and DG/CA<sub>2/3</sub>

subregions were segmented. Dentate gyrus (DG), CA<sub>2</sub>, and CA<sub>3</sub> regions were grouped into a single ROI as these regions cannot be reliably segmented at this particular resolution and MRI field strength (see Carr et al., 2010). Likewise, the CA fields were not clearly distinguishable in the most anterior (head) and posterior (tail) portions of the hippocampus; subregions were not defined within these ROIs, though they were included in collapsed anterior and posterior segments described below (Figs. 1 and 2). The magnitude of H.C.’s volume reduction combined with an unusual shape of H.C.’s hippocampus presented a somewhat unique challenge for subregion segmentation using the landmarks and geometric features typically present in controls. For example, the most typical shape of the hippocampal body is an ellipsoid, oblong in the medial-to-lateral dimension, though there is some variation of this shape among controls. In H.C., a more extreme variant on this shape was observed, especially in slices near the midpoint along the

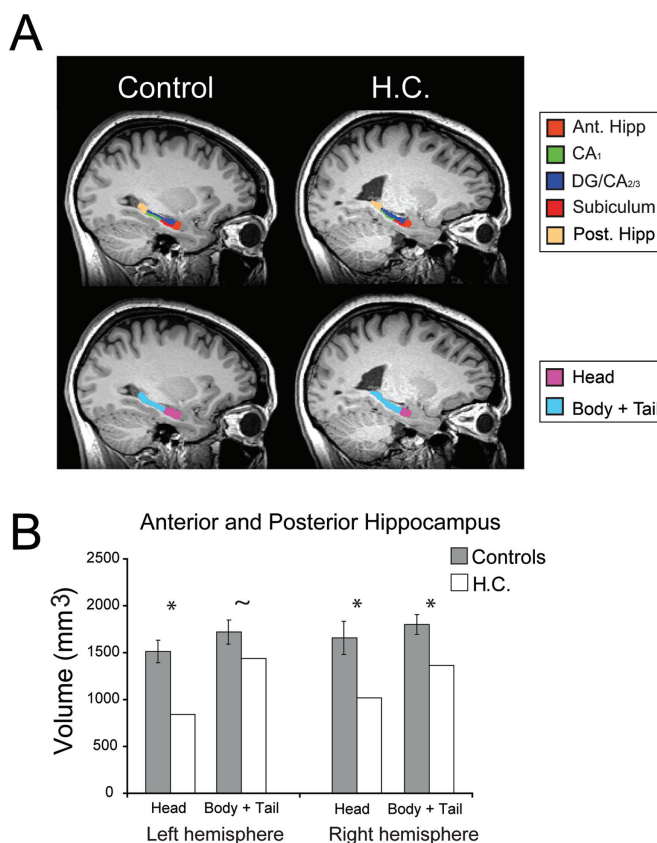


**FIGURE 1.** Anterior and posterior hippocampal volumes in H.C. and controls. **A:** A sagittal view of both a representative control participant along with H.C.’s left hippocampus. The upper panel displays the hippocampal subregions, which were manually traced on the T2-weighted image (see Fig. 2) and then co-registered to the T1-weighted image for visualization purposes. These subregions were combined into a single ROI and then split into anterior and posterior segments. The lower panel depicts the anterior segment (hippocampal head) in pink and the posterior portion (body and tail) in aqua. **B:** Anterior and posterior hippocampal volumes for H.C. (white bars) and the ten control participants (grey bars). Error bars reflect 95% confidence, \* refers to *P*-values < 0.05, and ~ demarcates *P*-values < 0.1 in all plots.

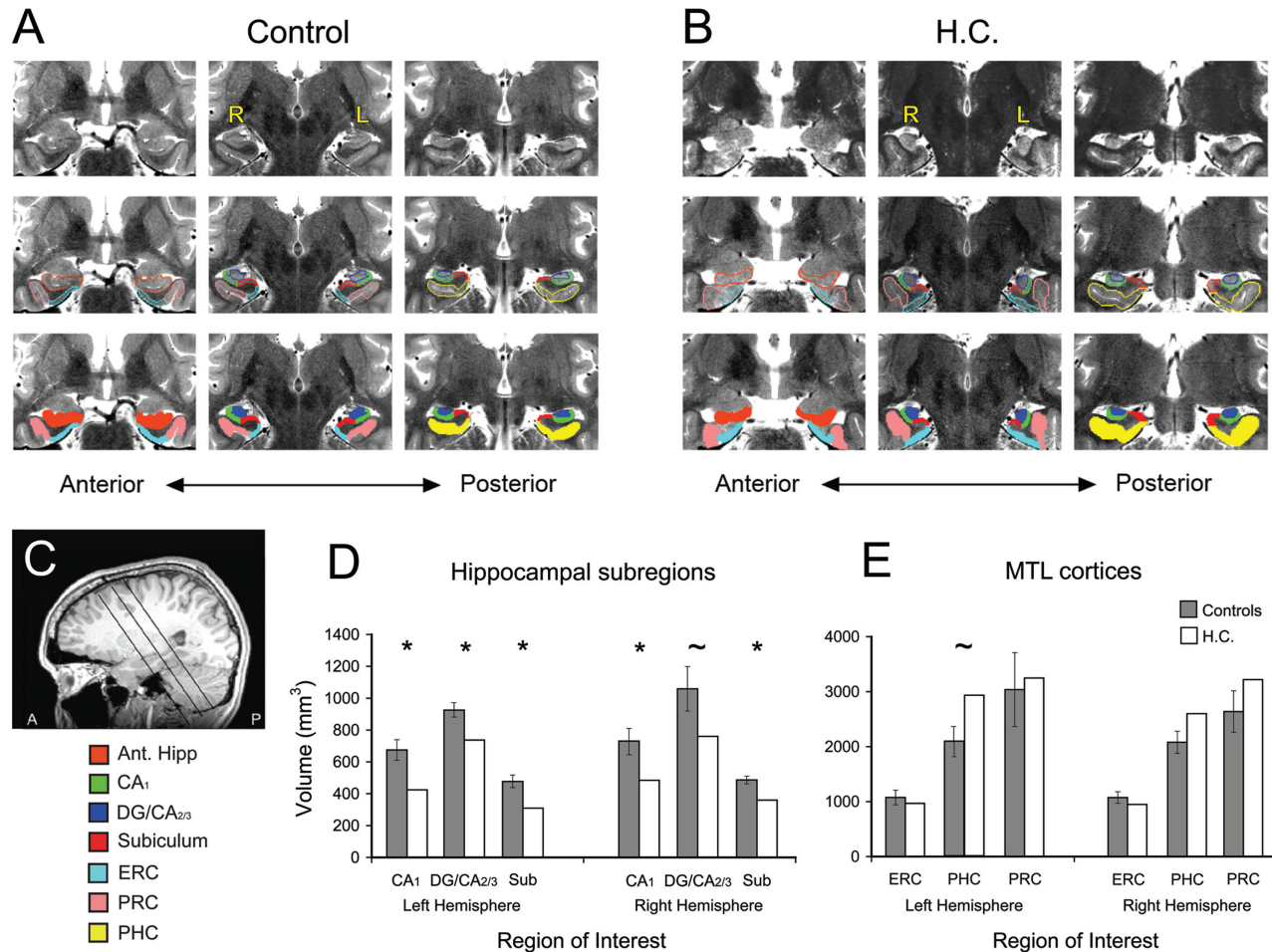


**FIGURE 2.** Segmentation of hippocampal and MTL cortex subregions in H.C. and controls. Three coronal slices of the T2-weighted image for a representative control participant (A) and for H.C. (B). Upper row of A and B displays the MTL region without any tracings; the middle row depicts the outline of each ROI; ROI masks are overlaid on T2-weighted image the bottom row. C. Sagittal slice depicting approximate locations of the oblique coronal slices depicted in A and B. D. Average volumes plotted for each hippocampal subregion ROI for H.C. (white bars) and controls (grey bars). Note that the subregion volumes are restricted to the body of the hippocampus. E. MTL cortical volumes for H.C. and control participants.

Sagittal slice depicting approximate locations of the oblique coronal slices depicted in A and B. D. Average volumes plotted for each hippocampal subregion ROI for H.C. (white bars) and controls (grey bars). Note that the subregion volumes are restricted to the body of the hippocampus. E. MTL cortical volumes for H.C. and control participants.

anterior-posterior axis of the left hippocampus (Figure 2B). While most of the standard landmarks were still applicable, to accommodate this geometric transformation of the hippocampus, the transition between the CA<sub>1</sub> and CA<sub>2/3</sub> regions was drawn at the most superior-lateral “corner” of the hippocampus, instead of just beyond the curve on the superior section. Furthermore, in H.C. and also in controls in which normal image variation changed the visibility of anatomical landmarks, care was taken to reference adjacent slices in which landmarks were more visible, and a smooth transition in the borders among regions was achieved. The MTL cortices, including perirhinal cortex (PRC), entorhinal cortex (ERC), and parahippocampal cortex (PHC), were also segmented (Fig. 2). The subregions for the entire length of the hippocampus were then combined to form a complete hippocampus ROI for each hemisphere. Next, this ROI was divided into anterior and posterior segments, in which the anterior segment included the head of the

hippocampus extending posteriorly until the disappearance of the uncus apex (Weiss et al., 2005). The posterior segment included both the body and the tail of the hippocampus.

To account for potential differences in head size, a measure of brain volume was extracted to “correct” for head size variation using an adapted version of the ANIMAL algorithm (Collins et al., 1995). Brain volume was accounted for in each ROI using a regression-based technique; where each ROI is regressed on brain volume (collapsed across groups), the residual value (i.e., the structures actual size minus its predicted value based on the individual’s brain volume) is accounted for in each ROI for each individual (Free et al., 1995; NHSV = OHSV - Grad\* (BV<sub>i</sub> - BV<sub>mean</sub>), where NHSV is the corrected hippocampal subregion volume, OHSV is original hippocampal subregion volume, Grad is the gradient of the regression line between the hippocampal subregion volume and the brain volume measure, BV<sub>i</sub> is the brain volume measurement for that subject, and BV<sub>mean</sub> is the mean brain

volume for all subjects.) All measurements reported below are adjusted using this method. No significant difference in brain volume was observed between H.C. and controls ( $P = 0.20$ ).

Ratings of intra-rater reliability were established by comparing segmentations performed on five randomly selected control participants' segmented volumes which were repeated by the first author with a 1–6 month interval between first and second segmentations. To establish inter-rater reliability, five randomly selected control participants' segmented volumes were compared with that of a second rater. Both intra-rater and inter-rater reliability was calculated using the DICE overlap metric, which produces an overlap measure between 0 and 1, where 0 signifies no overlap and 1 is a perfect match (Dice, 1945). The intra-rater and inter-rater reliability results (Table 1) are typical of those reported in the literature for manual segmentations of hippocampal subregions and MTL cortex (Bonnici et al., 2012). To assess volume differences between the groups, volumes for each ROI (based on a single set of tracings by the first author) were computed. Bayesian hypothesis testing (Crawford & Garthwaite, 2007) was used; one-tailed  $t$ -tests were applied within the hippocampus, and two-tailed  $t$ -tests were applied within the MTL cortex.

As expected, overall hippocampal volume in H.C. was reduced compared to that of controls (Fig. 1). In right hippocampus, both anterior and posterior segments were significantly smaller in H.C. (anterior:  $P = 0.018$ ; posterior:  $P = 0.010$ ). In left hippocampus, the anterior portion of the hippocampus was significantly reduced and the posterior segment was marginally reduced in H.C. (anterior:  $P = 0.002$ ; posterior:  $P = 0.085$ ). While the bilateral reduction in anterior hippocampus volume was greater compared to the posterior segments, there was no significant dissociation between these two measures ( $P = 0.202$ ).

In the body of the hippocampus, significant group differences were found bilaterally in CA<sub>1</sub> (left:  $P = 0.013$ ; right:  $P = 0.032$ ) and subiculum (left:  $P = 0.008$ ; right:  $P = 0.003$ ), and on the left in DG/CA<sub>2/3</sub> ( $P = 0.009$ ). The right DG/CA<sub>2/3</sub> region was marginally smaller in H.C. ( $P = 0.090$ ). In the MTL cortex, no significant groups differences were observed within ERC (left:  $P = 0.600$ ; right:  $P = 0.424$ ) or PRC (left:  $P = 0.834$ ; right:  $P = 0.320$ ); however, left PHC volume was

marginally increased in H.C. compared to controls (left:  $P = 0.056$ ; right  $P = 0.108$ ).

In addition to the detailed MTL volumetrics, the current scanning protocol also enabled qualitative analysis of the integrity of other memory structures that has not been described before in DA, namely the mammillary bodies and fornix. A detailed slice-by-slice visual inspection on coronal and axial views of the whole brain 3D T1-weighted image by a neuroradiologist indicated atrophy of the fornix bilaterally and agenesis of the mammillary bodies.

In summary, these results confirm that hippocampal volume in H.C. is reduced, bilaterally, and that the adjacent MTL cortices are of normal volume. H.C.'s total hippocampal volume measurements (left = 2270.49 mm<sup>3</sup>, right = 2364.08 mm<sup>3</sup>) correspond with previous reported values (case E6 in Vargha-Khadem et al., 2003). However, the control group hippocampal volume measurements in the current study are smaller than those reported previously, which alters the volume reduction percentage for H.C. While it was previously assumed that H.C.'s hippocampal volume reduction was approximately 45% compared to controls (case D6 in Adlam et al., 2005; Hurley et al., 2011), the current investigation, which employed a control group matched specifically to H.C.'s demographics as opposed to one matched to a larger group of individuals with DA, indicated that her volume reduction may be closer to 29.5% on the left and 31.2% on the right.

This is the first investigation to directly quantify the extent and distribution of hippocampal volume loss in an individual with DA. The current results indicate that perinatal anoxia in humans affects both anterior and posterior segments of the hippocampus. CA<sub>1</sub> and DG/CA<sub>2/3</sub> subregion volumes are reduced in both hemispheres, but to a greater extent on the left. Furthermore, the subiculum, the major output structure of the hippocampus, was significantly reduced in both hemispheres. The unusual shape of H.C.'s left hippocampus has been described as "incomplete hippocampal inversion" or "hippocampal malrotation." While there is some evidence that this developmental variant is more prevalent in individuals with epilepsy (Gamss et al., 2009), others have argued that this variant can be observed in as high as 18% of the non-epileptic population and is therefore not an etiological factor in epilepsy (Bajic et al., 2009). To the best of our knowledge, H.C. has never suffered an epileptic seizure; instead, this case would suggest that incomplete hippocampal inversion is linked to a general disturbed brain development.

While investigation of the fornix and mammillary bodies was not the focus of this investigation, the neuroradiological assessment noted significant abnormalities in these structures, similar to those described in an adult-onset case of anoxia (Warren et al., 2012). In the future, quantification through diffusion tract tracings will likely yield important insights into the extent that these structures are damaged in DA, and in turn, the effect of this damage on behavior.

Functional circuits within the MTL exhibit differential developmental profiles (Jabès et al., 2011). The methods employed here do not allow for investigation of the individual cell-rich layers within hippocampal/MTL subregions (e.g., granule cell layer of the DG) and those that primarily contain

TABLE 1.

Dice Values for Intra-rater and Inter-rater Reliability for the Hippocampal Subregions

Subregion	Intra-rater		Inter-rater	
	Left	Right	Left	Right
CA <sub>1</sub>	0.83	0.77	0.76	0.70
DG/CA <sub>2/3</sub>	0.85	0.85	0.84	0.81
Subiculum	0.80	0.76	0.70	0.67
PRC	0.78	0.78	0.73	0.77
ERC	0.81	0.77	0.69	0.72
PHC	0.89	0.87	0.78	0.83

connections (e.g., stratum lacunosum-moleculare). The volumetric reductions observed in H.C. may thus reflect a reduction in neuronal size or number, reduced connections among cells, or some combination of both.

Case studies of individuals with amnesia, along with careful characterization of the individuals' brain damage, have contributed significantly to our current understanding of the organization of memory and hippocampal function (Squire & Zola, 1996; Vargha-Khadem et al., 1997). In the case of H.C., the relatively uniform volume reduction of hippocampal subregions and along the long axis of the hippocampus, together with MTL cortices of normal volume, might explain seemingly unique aspects of her cognitive profile. For example, though familiarity was found to be numerically better than recollection in H.C., as in other DA cases, her familiarity on Remember-Know recognition memory was significantly below that of healthy controls (Rosenbaum et al., 2011). Thus, it is possible that perirhinal cortex, though volumetrically normal, is not intact. Alternatively, H.C.'s familiarity impairment may relate to another area of compromise, such as difficulties in online semantic processing. The latter is suggested by additional impairment in public event memory (Rosenbaum et al., 2011) and short-term memory for novel material (Rose et al., 2012). By contrast, H.C.'s autobiographical episodic memory and future imagining have been found to range from intact to impaired (Kwan et al., 2010; Hurley et al., 2011), but are well above what has been seen in adult-onset amnesic cases (e.g., Rosenbaum et al., 2008), possibly due to remaining tissue in all subregions and/or reorganization of brain function. Thus, in conjunction with animal lesion studies (Kesner & Goodrich-Hunsaker, 2010), and investigations using high-resolution fMRI (Carr et al., 2010), future case studies of individuals with selective hippocampal damage will provide invaluable converging evidence, enabling a refinement of theories of hippocampal subregion function.

## Acknowledgments

We thank Robert S. C. Amaral for the segmentation of the five participants for the calculation of inter-rater reliability and Dr. Fuqiang Gao for his detailed neuroradiological analysis of the T1-weighted MRI. We also thank Nick Qiu, and Drs. Melissa Pangelinan, Erin Dickie, and M. Mallar Chakravarty for assistance with the whole-brain automated segmentation pipeline.

## REFERENCES

- Adlam AR, Vargha-khadem F, Mishkin M, Haan M De. 2005. Deferred imitation of action sequences in developmental amnesia. *J Cogn Neurosci* 17:240–248.
- Baddeley A, Vargha-Khadem F, Mishkin M. 2001. Preserved recognition in a case of developmental amnesia: Implications for the acquisition of semantic memory? *J Cogn Neurosci* 13:357–369.
- Bajic D, Kumlien E, Mattsson P, Lundberg S, Wang C, Raininko R. 2009. Incomplete hippocampal inversion-is there a relation to epilepsy? *Eur Radiol* 19(10):2544–2550.
- Bonnici HM, Chadwick MJ, Kumaran D, Hassabis D, Weiskopf N, Maguire E. a. 2012. Multi-voxel pattern analysis in human hippocampal subfields. *Front Hum Neurosci* 6:290.
- Carr VA, Rissman J, Wagner AD. 2010. Review imaging the human medial temporal lobe with high-resolution fMRI. *Neuron* 65:298–308.
- Collins DL, Holmes CJ, Peters TM, Evans AC. 1995. Automatic 3-D model-based neuroanatomical segmentation. *Hum Brain Mapp* 3:190–208.
- Crawford JR, Garthwaite PH. 2007. Comparison of a single case to a control or normative sample in neuropsychology: Development of a Bayesian approach. *Cogn Neuropsychol* 24:343–372.
- Dice LR. 1945. Measures of the amount of ecologic association between species. *Ecology* 26:297–302.
- Duvernoy HM. 2005. The human hippocampus: Functional anatomy, vascularization, and serial sections with MRI. New York: Springer.
- Free SL, Bergin PS, Fish DR, Cook MJ, Shorvon SD, Stevens JM. 1995. Methods for normalization of hippocampal volumes measured with MR. *Am J Neuroradiol* 16:637–643.
- Gamss RP, Slasky SE, Bello J. a, Miller TS, Shinnar S. (2009). Prevalence of hippocampal malrotation in a population without seizures. *Am J Neuroradiol* 30(8):1571–1573.
- Hurley N, Maguire E, Vargha-Khadem F. 2011. Patient HC with developmental amnesia can construct future scenarios. *Neuropsychologia* 49:3620–3628.
- Insausti R, Juottonen K, Soininen H, Insausti AM, Partanen K, Vainio P, Laakso MP, Pitka A. 1998. MR volumetric analysis of the human entorhinal, perirhinal, and temporopolar cortices. *Am J Neuroradiol* 19:659–671.
- Jabès A, Lavenex PB, Amaral DG, Lavenex P. 2011. Postnatal development of the hippocampal formation: A stereological study in macaque monkeys. *J Comp Neurol* 519:1051–1070.
- Kawasaki K, Traynelis SF, Dingledine R. 1990. Different responses of CA1 and CA3 regions to hypoxia in rat hippocampal slice. *J Neurophysiol* 63:385–394.
- Kesner RP, Goodrich-Hunsaker NJ. 2010. Developing an animal model of human amnesia: The role of the hippocampus. *Neuropsychologia* 48:2290–2302.
- Kwan D, Carson N, Addis DR, Rosenbaum RS. 2010. Deficits in past remembering extend to future imagining in a case of developmental amnesia. *Neuropsychologia* 48:3179–3186.
- Mueller SG, Stables L, Du a T, Schuff N, Truran D, Cashdollar N, Weiner MW. 2007. Measurement of hippocampal subfields and age-related changes with high resolution MRI at 4T. *Neurobiol Aging* 28:719–726.
- Olsen RK, Nichols EA, Chen J, Hunt JF, Glover GH, Gabrieli JDE, Wagner AD. 2009. Performance-related sustained and anticipatory activity in human medial temporal lobe during delayed match-to-sample. *J Neurosci* 29:11880–11890.
- Poppenk J, Evensmoen HR, Moscovitch M, Nadel L. 2013. Long-axis specialization of the human hippocampus. *Trends Cogn Sci* 17:230–240.
- Pruessner JC, Köhler S, Crane J, Lord C, Byrne A, Kabani N, Collins DL, Evans AC. 2002. Entorhinal and parahippocampal cortex from high-resolution MR images?: Considering the variability of the collateral sulcus. *Cereb Cortex* 12:1342–1353.
- Rosenbaum RS, Carson N, Abraham N, Bowles B, Kwan D, Köhler S, Svoboda E, Levine B, Richards B. 2011. Impaired event memory and recollection in a case of developmental amnesia. *Neurocase* 17:394–409.
- Rosenbaum RS, Moscovitch M, Foster JK, Schnyer DM, Gao F, Kovacevic N, Verfaellie M, Black SE, Levine B. 2008. Patterns of autobiographical memory loss in medial-temporal lobe amnesic patients. *J Cogn Neurosci* 20:1490–1506.

- Squire LR, Zola SM. 1996. Structure and function of declarative and non-declarative memory systems. *Proc Natl Acad Sci USA* 93:13515–13522.
- Vargha-Khadem F, Gadian DG, Watkins KE, Connelly a, Van Paesschen W, Mishkin M. 1997. Differential effects of early hippocampal pathology on episodic and semantic memory. *Science* 277:376–380.
- Vargha-Khadem F, Salmond CH, Watkins KE, Friston KJ, Gadian DG, Mishkin M. 2003. Developmental amnesia: Effect of age at injury. *Proc Natl Acad Sci USA* 100:10055–10060.
- Warren DE, Duff MC, Magnotta V, Capizzano A a, Cassell MD, Tranel D. 2012. Long-term neuropsychological, neuroanatomical, and life outcome in hippocampal amnesia. *Clin Neuropsychol* 26:335–369.
- Weiss AP, Dewitt I, Goff D, Ditman T, Heckers S. 2005. Anterior and posterior hippocampal volumes in schizophrenia. *Schizophr Res* 73:103–112.
- Yushkevich P a, Avants BB, Pluta J, Das S, Minkoff D, Mechanic-Hamilton D, Glynn S, Pickup S, Liu W, Gee JC, Grossman M, Detre J. a. 2009. A high-resolution computational atlas of the human hippocampus from postmortem magnetic resonance imaging at 9.4 T. *NeuroImage* 44:385–398.
- Zola-Morgan S, Squire LR, Amaral DG. 1986. Human amnesia and the medial temporal region: Enduring memory impairment following a bilateral lesion limited to field CA1 of the hippocampus. *J Neurosci* 6:2950–2967.